



Contents lists available at ScienceDirect

Radiation Measurements

journal homepage: www.elsevier.com/locate/radmeas

Out-of-field dosimetry and 2nd cancer risk assessment of child patients under proton therapy using a TLD-based microdosimeter

Bhaskar Mukherjee ^{a, b, *}, Carolina Fuentes ^b, Jamil Lambert ^b

^a School of Physics (A28), The University of Sydney, NSW 2006, Australia

^b West German Proton Therapy Centre Essen, Hufeland Straße 55, D-45147 Essen, Germany

HIGHLIGHTS

- A polystyrene phantom bombarded with energetic proton beams from a cyclotron.
- TLD-700/BeO pairs and a TEPC exposed to secondary radiation field.
- H, L_{av} and Q were evaluated as functions of TLGC area ratio.
- Calibrated TLD chips were placed on o-o-f organ locations of child patients.
- LAR of the 2nd cancer was calculated using TLD results and risk factors.

ARTICLE INFO

Article history:

Received 19 September 2016

Received in revised form

15 February 2017

Accepted 24 April 2017

Available online xxx

Keywords:

Out-of-field organs

Paediatric proton therapy

Passive microdosimeter

2nd cancer risk

Thermoluminescence dosimeter

Tissue equivalent proportional counter

ABSTRACT

A passive microdosimeter based on TLD-700 ($^7\text{LiF: Mg,Ti}$) and BeO chips was used to assess the dose equivalent (H), average LET (L_{av}) and quality factor (Q) of secondary radiations at out-of-field organs of child patients undergoing proton therapy. Six sets of microdosimeters were cross calibrated using a gas-filled tissue equivalent proportional counter (TEPC) exposed to stray radiation field produced by bombarding a polystyrene plate phantom (30 cm \times 30 cm \times 40 cm) with therapeutic proton beam of energies 81, 119, 150, 177, 201 and 231 MeV. The resulting H, L_{av} and Q were presented as linear functions of TL glow curve area ratio ($A_{\text{BeO}}/A_{\text{TLD700}}$) of the dosimeters pairs evaluated using a common TLD reader. Subsequently, the calibrated microdosimeters were attached to the locations of thyroid, left and right breast/lung and stomach of two child cancer patients of interest. After the completion of therapeutic proton exposure the TLD chips were removed from the child's body, read out and the values of H, L_{av} and Q at relevant organ locations evaluated. Using the organ, gender and age specific risk coefficients (R^T) the lifetime attributable risks of the 2nd cancer (LAR^T) were calculated.

© 2017 Elsevier Ltd. All rights reserved.

1. Introduction

During proton therapy (PT) high-energy proton beams deliver well-defined conformal therapeutic dose within the primary tumour volume, thereby reducing unwanted radiation exposure to the neighbouring healthy tissue. This unique merit endows significant therapeutic advantages to PT in comparison to conventional photon-therapy. However, a significant number of secondary particles, predominantly fast neutrons and photons, are produced by the interaction of the proton beam with the beam shaping and

modifying devices located inside the nozzle as well as from irradiated tumour mass itself (DeLancy and Kooy, 2008). This results in an unwanted increase in the radiation exposure to sensitive organs remote to treated tumour volume, thereby escalating the risk of second cancer. Due to smaller body size and higher radio sensitivity of organs (tissue) of interest the risk of the 2nd cancer (Hall, 2006; Harrison, 2013) is higher in child patients (Athar and Paganetti, 2011).

Under the framework of Working group (WG) 9 of European Radiation Dosimetry (EURADOS) group researchers have characterized the stray radiation fields around a tissue-equivalent target bombarded with therapeutic proton beam using a myriad of radiation detectors. The experimental results were also validated with elaborate Monte Carlo simulations (Farah et al., 2015). Researchers irradiated a simulated ocular-melanoma of an adult

* Corresponding author. School of Physics (A28), The University of Sydney, NSW 2006, Australia.

E-mail address: bhamukh@gmail.com (B. Mukherjee).

anthropomorphic (RANDO) phantom as well as a computational phantom (ADAM) with 60 MeV single scattered proton beam from a medical cyclotron. They have primarily used Thermoluminescent Dosimeters (TLD), Polyallyl-Diglycol-Carbonate (PADC) track etch detectors and Monte-Carlo technique to calculate the fatal 2nd cancer risk in seven critical out of field (o-o-f) organs (Stolarczyk et al., 2011).

A solid state SOI (Silicon on Insulator)-microdosimeter was developed and implemented to assess important microdosimetric parameters at (o-o-f) regions of an adult anthropomorphic phantom made of Lucite, whereas the simulated target (prostate gland) was irradiated with energetic proton beam (Wroe et al., 2007). The relatively large physical size and requirement of live electrical power and data-transfer interface prevent those electronic detectors to be precisely positioned at the location of (o-o-f) organs of interest of patients in particular, paediatric subjects undergoing proton therapy. These make their applications in-vivo dosimetry in clinical environment unfeasible.

A tiny microdosimeter based on widely used TLD-700 and BeO dosimeter chips (Mukherjee, 2015) was used to circumvent the above shortcomings. The derived microdosimetric quantities; average LET (L_{av}), Quality Factor (Q) and dose equivalent (H) were implemented to estimate the lifetime attributable (organ specific) second cancer risk (LAR) of child patients undergoing proton therapy. Dosimetry methods and risk assessment of the 2nd cancer is reviewed in the reference (Harrison, 2013). Potential applications of microdosimetry in particle therapy related fields are highlighted in the literature (Wambersie et al., 2015).

2. Materials and methods and data analysis

2.1. Operation principles and calibration of TLD microdosimeter

The ratio of thermoluminescent signal output (TL-glow curve area) of Beryllium Oxide (BeO) and Lithium Fluoride (${}^7\text{LiF}$: Mg,Ti) chips ($A_{\text{BeO}}/A_{\text{LiF}}$) increases with rising linear energy transfer (LET) of the impinging particles on the dosimeter pairs. Secondary radiation fields with varying radiation quality and LET distributions were generated by bombarding a polystyrene plate phantom (PPP) (30 cm \times 30 cm \times 40 cm) with 81, 119, 150, 177, 201 and 231 MeV proton beam in uniform scanning (US) mode from the PROTEUS 235 Medical Cyclotron operated by the West German Proton Therapy Centre Essen (WPE), Germany. The researchers accomplished the shaping of the proton-beam using a 50 mm thick brass aperture with a 70 mm \times 70 mm rectangular slot (Fig. 1a). They have not utilised any extra beam modifying devices like range shifter, bolus or ridge filter (Mukherjee, 2015). The corresponding ranges of the proton beam in water ($R_{\text{H}_2\text{O}}$) were calculated to be 5, 10, 15, 20, 25, and 32 cm respectively. The representation of proton beam energy in terms of water equivalent range is required by the mandatory Quality Assurance (QA) protocol (DeLancy and Kooy, 2008). A proton dose of 50 Gy (5000 Monitor Unit) at a dose rate of 2 Gy min^{-1} was delivered to PPP in all six cases. Pairs of TLD-700 and BeO chips were attached to a gas-filled spherical (60 mm diameter) Rossi-Type Tissue Equivalent Proportional Counter (TEPC- Model: REM500B, Manufacturer: Health Physics Instruments, Goleta, CA 93117, USA). The TEPC was positioned at contact with the lateral wall of the PPP and aligned to the energy depended stopping range R of the proton beam. The air gap (A) between the beam exit (Nozzle) and entrance (PPP) planes was kept fixed at 20 cm. After the completion of each run, i.e. proton bombardment of the PPP the TEPC (including attached TLD pairs) was removed from the treatment room for evaluation. Subsequently a new TLD pair was attached to TEPC and the irradiation procedure was repeated (Fig. 1a, b). The TLD glow curves and TEPC

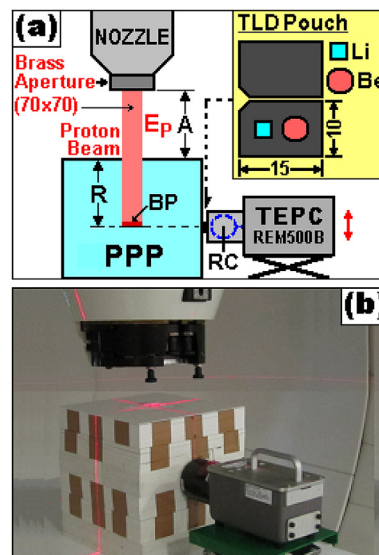


Fig. 1. (a) Principle of TLD Microdosimeter calibration set up showing the polystyrene plate phantom (PPP), proton beam of energy E_p passing through brass aperture with a 70 mm \times 70 mm rectangular slot and the REM500B TEPC (housing a 60 mm diameter spherical Rossi Counter RC) with the TLD pouch pairs attached to it. The air gap (A) was kept fixed at 20 cm. The proton beam sharply stops at Bragg Peak zone (BP). The schematic diagram of the pouch (10 mm \times 15 mm) made of four wraps of thin (~ 0.15 mm) light tight (black) Mylar foil containing TLD-700 (Li) and BeO (Be) dosimeter pairs is shown inset. (b) Photograph of the calibration set up showing the PPP and TEPC placed under the beam delivery nozzle situated in the patient treatment room.

readouts were used to calibrate the microdosimeter (Mukherjee, 2015).

2.2. Evaluation of TLD microdosimeter

After the completion of radiation exposure the TEPC was removed from treatment room and interfaced to a PC. The stored data was downloaded and LET spectrum (Fig. 2a) evaluated. The average LET (L_{av}), Quality Factor (Q) and dose equivalent (H) were also derived (Liu, 2000). The glow curves of BeO and TLD-700 chips were evaluated using a manual TLD reader (Model: M3500, Manufacturer: Thermo-Fisher, Erlangen, Germany) at a heating rate of 5 $^\circ\text{Cs}^{-1}$. The temperature interval of integrated TL glow curve (TLGC) area was (100–210 $^\circ\text{C}$) and (100–250 $^\circ\text{C}$) for BeO and TLD-700 respectively (Fig. 2b). The results are summarised in Table 1. The calibration parameters relevant to average LET (L_{av}), Q, H and dose equivalent conversion factor h_H are presented as following linear regression functions (Mukherjee, 2015):

$$L_{av} \text{ (keV}/\mu\text{m}) = 261.0r - 25.3 \quad (1)$$

$$Q = 60.1r - 6.76 \quad (2)$$

$$h_H \text{ (mSv/nC)} = 2.14 \times 10^{-4} - 5.59 \times 10^{-4}r \quad (3)$$

$$H \text{ (mSv)} = h_H A_{\text{LiF}} \quad (4)$$

where, r and A_{LiF} (nC) represent the TL glow curve area ratio ($A_{\text{BeO}}/A_{\text{LiF}}$) of BeO and TLD-700 dosimeters and glow curve area of TLD-700 respectively (Fig. 2b). The data points were taken from columns 6 and 7 of Table 1.

It is worthwhile to note that high-energy protons (Table 1, Column 1) were used to produce secondary particles of with a wide LET distribution by bombarding the PPP (Mukherjee, 2015), for

Download English Version:

<https://daneshyari.com/en/article/8250339>

Download Persian Version:

<https://daneshyari.com/article/8250339>

[Daneshyari.com](https://daneshyari.com)